

High-spin states in $^{97,98}\text{Rh}$

S. S. Ghugre,* B. Kharraja,† and U. Garg

Department of Physics, University of Notre Dame, Notre Dame, Indiana 46556

R. V. F. Janssens, M. P. Carpenter, B. Crowell,‡ T. L. Khoo, T. Lauritsen, and D. Nisius

Physics Division, Argonne National Laboratory, Argonne, Illinois 60439

W. Mueller,§ W. Reviol, and L. L. Riedinger

Department of Physics, University of Tennessee, Knoxville, Tennessee 37996

R. Kaczarowski

Soltan Institute for Nuclear Studies, 05-400 Swierk, Poland

(Received 7 July 1998)

High-spin states in $^{97,98}\text{Rh}$ ($Z=45$) were populated via the $^{65}\text{Cu}(^{36}\text{S},xn)^{97,98}\text{Rh}$ ($x=4,3$) fusion-evaporation reactions. More than 40 additional transitions have been identified and placed in the decay schemes of these nuclei. The level scheme of ^{97}Rh has been extended up to tentative spins of $J^\pi = 39/2^+, 37/2^-$, and the placement of some of the previously known transitions has been revised. The level structure of ^{97}Rh indicates a single-particle nature and the observed levels are reproduced well by spherical shell-model calculations. The level scheme of ^{98}Rh has been extended up to spins $J \sim 20\hbar$ and up to an excitation energy of ~ 10 MeV. The low-spin structure of ^{98}Rh ($J \leq 10\hbar$), appears to indicate also a single-particle structure, as supported by the stretched coupling scheme [$^{97}\text{Rh}(J') \otimes \nu(d_{5/2}) = ^{98}\text{Rh}(J)$]. [S0556-2813(98)03912-0]

PACS number(s): 27.60.+j, 23.20.Lv, 21.60.Cs

I. INTRODUCTION

Nuclei near and at the proton and neutron magic number 50 reveal a gradual change in structure as the number of nucleons moves further from the closed shell configuration. The low-lying states of nuclei near the $N=50$ shell exhibit a single-particle nature. However, collective quadrupole excitations begin to develop when the neutrons start filling the 50–82 valence orbitals, in particular the deformation driving neutron orbital $\nu h_{11/2}$. In the past few years, considerable effort has been devoted to the study of the high-spin-level structures of Ru ($Z=44$) and neighboring nuclei with $N \leq 51$ [1,2] and $N \geq 55$ [3]. Single-particle configurations dominate the level structures of nuclei with $N \leq 51$ even at high angular momenta ($J \approx 20\hbar$, $E_x \approx 10$ MeV) [2], whereas nuclei with $N \geq 55$ exhibit collective behavior [4]. Experimental information on the level structures of nuclei with $N=52-54$ has become available only recently [5,6].

In this paper, we report on our investigation of high-spin states in the “transitional” nuclei $^{97,98}\text{Rh}$ ($N=52,53$). This work is a continuation of efforts to understand the level structure of nuclei with neutron numbers $52 \leq N \leq 54$, and to search for the possible onset of collectivity [5,6]. It should be

noted that no collective structures have been observed either in the $N=52$ ^{94}Mo [6], ^{95}Tc [7], and ^{96}Ru [5] isotones, nor in the $N=53$ ^{95}Mo [6], ^{96}Tc [7], and ^{97}Ru [5] isotones. One aim of this work has been to study the effect of an extra proton on the microscopic structure of the $N=52$ and 53 isotones.

II. EXPERIMENTAL DETAILS

High-spin states in $^{97,98}\text{Rh}$ were populated via the $^{65}\text{Cu}(^{36}\text{S},xn)$ ($x=4,3$) reactions at a bombarding energy of 142 MeV. Although the incident beam energy was not optimized (according to statistical model calculations) for the $^{97,98}\text{Rh}$ reaction channels (γ rays from ^{97}Rh and ^{98}Rh accounted for only 4.7% and 3.5% of the total γ -ray flux, respectively), it was still possible to obtain substantial information on the higher-angular-momentum states in these nuclei. The ^{36}S beam was provided by the 88-in. cyclotron facility at the Ernest O. Lawrence Berkeley National Laboratory. Two stacked, self-supporting, isotopically enriched ^{65}Cu target foils (~ 0.5 mg/cm² thick) were used. Triple- and higher-fold coincidence events were measured using the early implementation phase of the Gammasphere array, which at that time comprised 36 Compton-suppressed Ge detectors. A total of about 400×10^6 events were accumulated and stored onto magnetic tapes for further analysis.

The data were sorted into three-dimensional histograms (E_γ - E_γ - E_γ cubes) using the RADWARE [8] and Kuehner [9] formats. The coincidence cube with the RADWARE format was analyzed with the RADWARE software package [8], which uses the generalized background subtraction algorithm of Ref. [10] to extract spectra corresponding to two coincidence gates (the so-called double-gated spectra). Such

*Present address: IUCDAEF Calcutta Center, Sector III/LB-8, Bidhan Nagar, Calcutta 700 091, India.

†On leave from Physics Department, University Chouaib Doukali, Boîte Postale 20, El Jadida, Morocco.

‡Present address: Fullerton Community College, Fullerton, CA 92833.

§Present address: Katholieke Universiteit Leuven, B-3000 Leuven, Belgium.

double-gated spectra were also obtained from the Kuehner cube using the FUL method of background subtraction [11]. The experimental details, including procedures for constructing level schemes and for multipolarity assignments, are the same as those outlined in Ref. [5]. In particular, multipolarity assignments were based primarily on intensity ratios extracted from angle-sorted matrices: Coincidence gates were placed on transitions detected in the forward-angle (32° and 37°) detectors and the γ rays measured at 90° and at backward angles (143° and 147°) were sorted along the two axes of the matrices. Although, as pointed out in Ref. [5], such directional correlation ratios $R = I_\gamma(\text{backward})/I_\gamma(90^\circ)$ have their limitations, reliable spin assignments can still be made by comparing the ratios for the new γ lines with those of previously known γ rays whose multipolarity is already firmly established. In the present configuration, γ rays of $E2$ character have $R \approx 1.9$, whereas dipole transitions have $R \approx 1.5$. Tables I and II list all γ rays assigned to ^{97}Rh and ^{98}Rh , respectively, along with their intensities, the intensity ratios R (where available), and the proposed placements in the level schemes.

III. RESULTS

A. Level scheme of ^{97}Rh

A representative double-gated spectrum for ^{97}Rh is shown in Fig. 1 and the level scheme of this nucleus, as obtained from the present experiment, is shown in Fig. 2. Prior to this work, the level structure of ^{97}Rh was known up to a spin of $J = (31/2)\hbar$ and an excitation energy of $E_x \approx 7$ MeV [12]. On the basis of the present work, 20 additional transitions have been placed in the decay scheme of ^{97}Rh , and the level scheme has been extended up to $J \approx 20\hbar$ and $E_x \approx 10$ MeV. The states below $J = (29/2)\hbar$ are in agreement with the previous work [12]. The transitions observed in the positive-parity structure have energies of 1075, 1180, 1396, 1457, 1563, 1690, 1812, 1820, 2068, and 2171 keV, respectively. In previous work [12], the 1258-keV transition had been placed parallel to the 1587-keV transition (1590 keV in the present work). Also, the 825- and 311-keV transitions were placed parallel to the 1134-keV transition. In the present work, the 1590-, 1258-, and 1242-keV transitions are found to be in coincidence with each other and to form a sequence and the 825- and 311-keV transitions are placed above the 6190-keV [$J = (35/2^+)$] level. The placement of the 674- and 1075-keV transitions is tentative, hence the dashed lines in the level scheme.

The negative-parity sequence is extended up to a spin of $J = (37/2)\hbar$ and an excitation energy of $E_x \approx 10$ MeV. The transitions belonging to this ‘‘band’’ are of energies 467, 499, 793, 1258, 1505, and 1543 keV, respectively. The proposed structure differs from the previous work [12,13] in that (i) Vanhorenbeck *et al.* [13] had observed an $E2$ cascade spanning the $1/2^-$ and $17/2^-$ states (this cascade is not observed in the present experiment) and (ii) an 1178-keV transition reported by Piel *et al.* [12] is not observed either and it appears that the intensities of the low-lying 409-, 656-, and 696-keV transitions were overestimated in that work, perhaps due to contamination from the ^{96}Ru and ^{98}Pd nuclei produced in the same reaction.

TABLE I. Energies, initial and final spins, relative intensities, and the DCO ratios R (as defined in the text) for transitions assigned to ^{97}Rh .

E_γ (keV) ^a	$J_i \rightarrow J_f$ ^b	I_γ ^c	R ^d
89.0	$17/2^+ \rightarrow 15/2^+$	10	1.6 (0.4)
164.0	$23/2^+ \rightarrow (21/2)^+$	3.9 (0.5)	
260.3	$29/2^+ \rightarrow 27/2^+$	20	1.5 (0.3)
290.7	$(23/2^-) \rightarrow (21/2^-)$	14.3 (1.0)	1.6 (0.3)
293.0	$25/2^+ \rightarrow 23/2^+$	16	1.6 (0.2)
310.9	$\rightarrow (35/2^+)$	9.4 (1.5)	
409.4	$19/2^+ \rightarrow 17/2^+$	61	1.5 (0.2)
464.8	$27/2^+ \rightarrow 25/2^+$	20	1.5 (0.2)
466.8	$(33/2^-) \rightarrow (31/2^-)$	7.2 (0.8)	1.5 (0.3)
498.7	$(33/2^-) \rightarrow (31/2^-)$	5.5 (1.0)	1.6 (0.4)
606.7	$15/2^+ \rightarrow 13/2^+$	30	1.6 (0.3)
642.2	$23/2^+ \rightarrow 21/2^+$	10	1.5 (0.2)
655.8	$21/2^+ \rightarrow 19/2^+$	24	1.6 (0.3)
672.9	$17/2^- \rightarrow 17/2^+$	5	
674.4	$(35/2^+) \rightarrow (33/2^+)$	≤ 1	
695.7	$17/2^+ \rightarrow 13/2^+$	70	2.1 (0.3)
725.1	$29/2^+ \rightarrow 25/2^+$	25	2.0 (0.2)
729.5	$(25/2^-) \rightarrow (23/2^-)$	7.2 (1.0)	1.5 (0.2)
757.6	$27/2^+ \rightarrow 23/2^+$	29	2.0 (0.3)
762.0	$17/2^- \rightarrow 15/2^+$	20.2 (1.0)	1.3 (0.2)
793.0	$(37/2^-) \rightarrow (35/2^-)$	≤ 1	
809.7	$31/2^+ \rightarrow 27/2^+$	28	1.9 (0.2)
815.0	$(31/2^-) \rightarrow (29/2^-)$	15.4 (1.0)	1.5 (0.2)
825.1	^e	3.0	
831.3	$(21/2^-) \rightarrow 17/2^-$	25	1.9 (0.3)
858.4	$13/2^+ \rightarrow 9/2^+$	100	2.0 (0.3)
935.2	$25/2^+ \rightarrow 21/2^+$	26	1.6 (0.3)
1020.2	$(25/2^-) \rightarrow (21/2^-)$	7	1.9 (0.3)
1065.2	$21/2^+ \rightarrow 17/2^+$	14	2.2 (0.3)
1075.0	^f	≤ 1	
1086.0	$(29/2^-) \rightarrow (25/2^-)$	22	1.9 (0.3)
1134.0	$(21/2^+) \rightarrow 19/2^+$	8	1.6 (0.3)
1180.0	$(39/2^+) \rightarrow (37/2^+)$	5	
1242.3	$(33/2^+) \rightarrow 29/2^+$	41	2.1 (0.2)
1258.3	$(37/2^+) \rightarrow (33/2^+)$	35	1.5 (0.3)
1257.9	$(35/2^-) \rightarrow (33/2^-)$	4.0 (1.1)	
1298.0	$23/2^+ \rightarrow 19/2^+$	30	2.1 (0.2)
1367.2	$(35/2^+) \rightarrow 31/2^+$	25	1.9 (0.2)
1395.9	$(35/2^+) \rightarrow (33/2^+)$	5	1.6 (0.2)
1457.0	$\rightarrow (33/2^+)$		
1505	$\rightarrow (35/2^-)$	≤ 1	
1508	$\rightarrow (37/2^+)$	≤ 1	
1543	$\rightarrow (35/2^-)$	≤ 1	
1563	$(35/2^+) \rightarrow (33/2^+)$	2.2 (0.5)	
1590	$(39/2^+) \rightarrow (37/2^+)$	9	1.5 (0.4)
1690	$(31/2^+) \rightarrow 29/2^+$	4	
1812	$\rightarrow (35/2^+)$	4.0 (2.0)	
1820	$\rightarrow (37/2^+)$	≤ 1	
2068	$\rightarrow (33/2^+)$	≤ 1	
2171	$\rightarrow (33/2^+)$	≤ 1	

^aThe transitions of energies ≤ 1500 keV are known to ~ 0.4 keV; for higher energies, the errors are ~ 1 keV.

^bThe J^π of the levels for which a DCO ratio R could not be extracted and are not fixed by other interband transitions are given in parenthesis.

^cExcept where stated, the uncertainties in intensities are less than 10%.

^dA blank space is kept for all the transitions for which no DCO ratio R could be obtained.

^eThe 825-keV transition feeds the 311-keV transition.

^fThe 1075-keV transition feeds the 1812-keV transition.

TABLE II. Energies, initial and final spins, relative intensities, and the DCO ratio R (as defined in the text) for transitions assigned to ^{98}Rh .

E_γ (keV) ^a	$J_i \rightarrow J_f$ ^b	I_γ ^c	R ^d
207.1	$8^+ \rightarrow$	5.0 (1.0)	
208.6	$\rightarrow (15^-)$	≤ 1	
216.3	$(9^-) \rightarrow 8^+$	11.0 (1.0)	1.2 (0.2)
219.1	$\rightarrow (13^+)$	4.0 (0.5)	
265.2	$(10^+) \rightarrow (9^+)$	23	1.6 (0.2)
409.2	_e	≤ 1	
413.4	$(8^+) \rightarrow 8^+$	6.0 (0.6)	
457.4	$(11^+) \rightarrow (9^+)$	8.5 (0.5)	2.2 (0.4)
463.4	$(10^-) \rightarrow (9^-)$	9.5 (1.0)	1.5 (0.3)
549.5	$(11^+) \rightarrow (10^+)$	23	1.5 (0.4)
650.7	$(17^+) \rightarrow (15^+)$	10	1.9 (0.3)
726.5	$6^+ \rightarrow 4^+$	84.2	1.8 (0.3)
792.5	$(11^-) \rightarrow (10^-)$	8.0 (2.2)	1.6 (0.3)
815.4	$(11^+) \rightarrow (9^+)$	30	2.1 (0.5)
831.4	$(10^+) \rightarrow 8^+$	18	2.0 (0.4)
841.6	$4^+ \rightarrow 2^+$	100	1.9 (0.3)
857.1	$(16^+) \rightarrow (15^+)$	4.0 (0.5)	
889.7	$(19^+) \rightarrow (17^+)$	6.8 (1.0)	2.1 (0.4)
933.1	$(13^-) \rightarrow (12^-)$	4.0 (1.0)	1.6 (0.3)
934.6	$(17^+) \rightarrow (16^+)$	4.0 (0.5)	
980.4	$9^+ \rightarrow 8^+$	58	1.5 (0.3)
995.1	$8^+ \rightarrow 6^+$	67	2.0 (0.2)
1096.0	$(21^+) \rightarrow (19^+)$	4.0 (1.0)	
1125.2	$(12^+) \rightarrow (11^+)$	5.1 (0.6)	1.6 (0.3)
1137.3	$(13^+) \rightarrow (11^+)$	41	2.1 (0.3)
1150.7	$\rightarrow (14^-)$	≤ 1	
1207.9	$(13^-) \rightarrow (12^-)$	2.5 (0.5)	
1287.6	$(14^-) \rightarrow (13^-)$	2.0 (0.8)	
1347.4	$(14^-) \rightarrow (13^-)$	2.0 (0.4)	
1363.9	$(15^+) \rightarrow (13^+)$	26	2.0 (0.3)
1380.9	$(12^-) \rightarrow (11^-)$	7.0 (1.0)	1.5 (0.2)
1409.4	$(8^+) \rightarrow 6^+$	13	2.2 (0.4)
1433.1	$(17^+) \rightarrow (15^+)$	4.0 (1.7)	
1435.9	$\rightarrow (12^-)$	2.1 (0.5)	
1487.5	$(15^-) \rightarrow (14^-)$	2.0 (1.2)	
1495	$(13^+) \rightarrow (11^+)$	8.0 (1.0)	2.2 (0.4)
1547	$(14^-) \rightarrow (12^-)$	2.0 (1.0)	

^aThe transitions of energies ≤ 1500 keV are known to ~ 0.4 keV; for higher energies, the errors are ~ 1 keV.

^bThe J^π of the levels for which the DCO ratio R could not be extracted and are not fixed by other interband transitions are given in parenthesis.

^cExcept where stated, the uncertainties in intensities are less than 10%.

^dA blank space is kept for all the transitions for which no DCO ratio R could be obtained.

^eThe 409-keV transition is fed by the 207-keV transition.

A number of γ rays with $E_\gamma \geq 1.5$ MeV appear at high spins [$J \geq (33/2^+)$], accompanied by a fragmentation of the intensity into several branches. This pattern has now been observed in many nuclei in this region and is indicative of the breaking of the $N=50$ core [5,6].

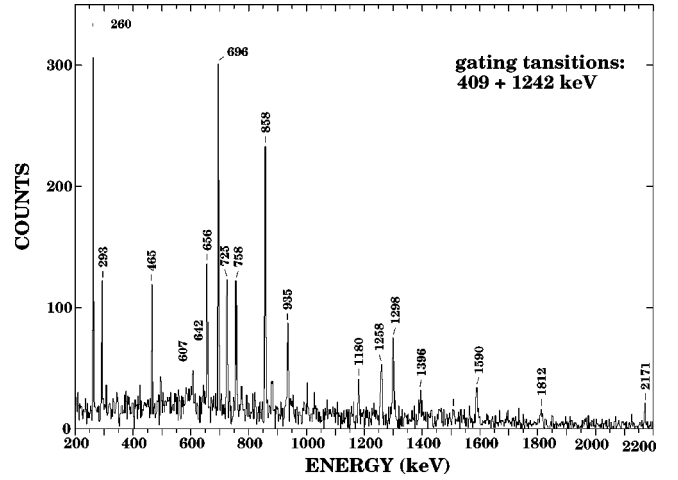


FIG. 1. Representative double-gated coincidence γ spectrum for ^{97}Rh . All energies are marked to within ± 1 keV. The spectrum shown has not been corrected for efficiencies of the Ge detectors.

B. Level scheme of ^{98}Rh

A typical double-gated projection for ^{98}Rh is shown in Fig. 3. Prior to the present work, only five members of a cascade based on the (2^+) ground state were known in ^{98}Rh [14]. The level structure (shown in Fig. 4) has now been extended up to a spin of $J=[(21^+), (14^-)]$ and an excitation energy of $E_x \approx 10$ MeV. The states are found to decay through two separate γ -ray cascades of opposite parity. The same behavior has been observed by Kharraja *et al.* in ^{96}Ru [5]. The transitions observed in the positive-parity band are of energies 219, 413, 457, 550, 651, 815, 831, 857, 890, 935, 1096, 1125, 1137, 1364, 1409, 1433, and 1495 keV, respectively. An $M1$ multipolarity has been assigned to the 980-keV transition on the basis of several crossover transitions present in that part of the level scheme; in earlier work, this transition had been assigned an $E2$ character [14].

A negative-parity cascade has also been observed and comprises transitions with energies of 409, 463, 793, 933, 1151, 1208, 1288, 1347, 1381, 1436, 1488, and 1547 keV, respectively. This cascade is built on the $J=9^-$ level and connects to the 8^+ and 6^+ levels via transitions of 216, 207, and 409 keV. There are indications in the coincidence relationships for the existence of connecting transitions between the positive and negative parity cascades at higher spins as well; however, due to the lack of statistics (^{98}Rh was one of the weakest channels populated in this reaction) these (evidently weak) transitions could not be observed.

A sequence of $E2$ transitions is built on the $J=9^+$ level. The energies of these transitions (815, 1136, 1364, and 1433 keV) increase monotonically with increasing spin and this sequence is reminiscent of a rotational band. However, no definite conclusion can be reached regarding the possible collective behavior manifested by this cascade in the absence of supporting evidence from, e.g., lifetime measurements.

In a contemporaneous investigation, ^{98}Rh has been studied using the $^{70}\text{Ge}(^{32}\text{S}, 3pn)^{98}\text{Rh}$ reaction [15]; the highest spins and excitation energies achieved therein are slightly lower than those in our work, however. The placement of most of the transitions reported in [15] are similar to our results. However, there are two important differences. First,

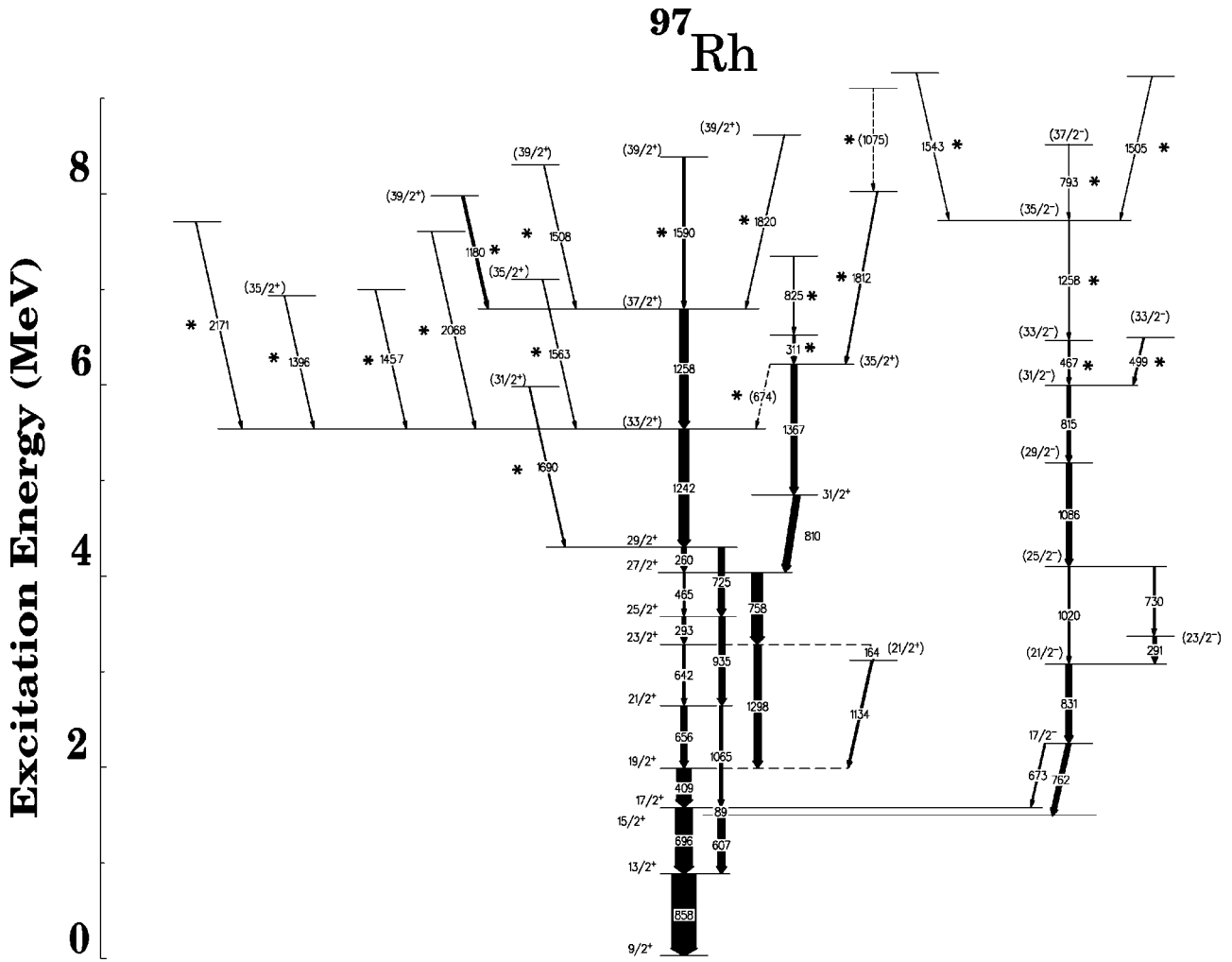


FIG. 2. Level scheme for ^{97}Rh as obtained from the present study. The transition energies are labeled in keV. The new transitions (as well as those with revised placements) are marked with an asterisk. The widths of the arrows are approximately equal to the relative intensities of the observed γ transitions.

the parity assignments for the structures above the 8^+ level are reversed. The argument in favor of a negative parity for the relevant structure in Ref. [15] stems from the fact that the 1409-keV transition has been assigned as $E1$, based on DCO ratio measurements and the partial branching ratio of the γ transitions deexciting the state ($I=7\hbar$). The DCO ratio for this transition in our measurements would suggest a quadrupole multipolarity ($E2$) instead. A similar discrepancy has been observed for the 815- and 1495-keV transitions: An $E2$ character is assigned to these γ rays based on DCO ratios and crossover transitions. The second discrepancy is the absence of the $E2$ cascade that was presented as a deformed band, together with the intermediate (connecting) $M1$ transitions in Ref. [15]. This sequence comprises $E2$ transitions of energies 1230, 1311, and 1485 keV, respectively, and the 681-, 455-, 856-, and 506-keV $M1$ transitions [15]. A very careful search for the transitions reported in this sequence, using many combinations of double-gated coincidence spectra combined with good statistics, ended with a null result. (A total of 400×10^6 greater than or equal to three-fold events, equivalent to more than 1200×10^6 twofold coincidence have been collected in the present work, of which approximately 42×10^6 events correspond to the ^{98}Rh

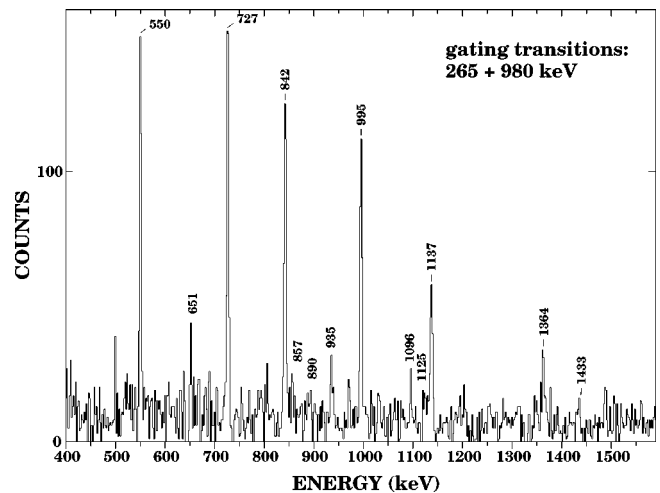


FIG. 3. Representative γ - γ - γ coincidence spectrum for ^{98}Rh for the indicated gates. All energies are marked to within ± 1 keV. The spectrum shown has not been corrected for efficiencies of the Ge detectors.

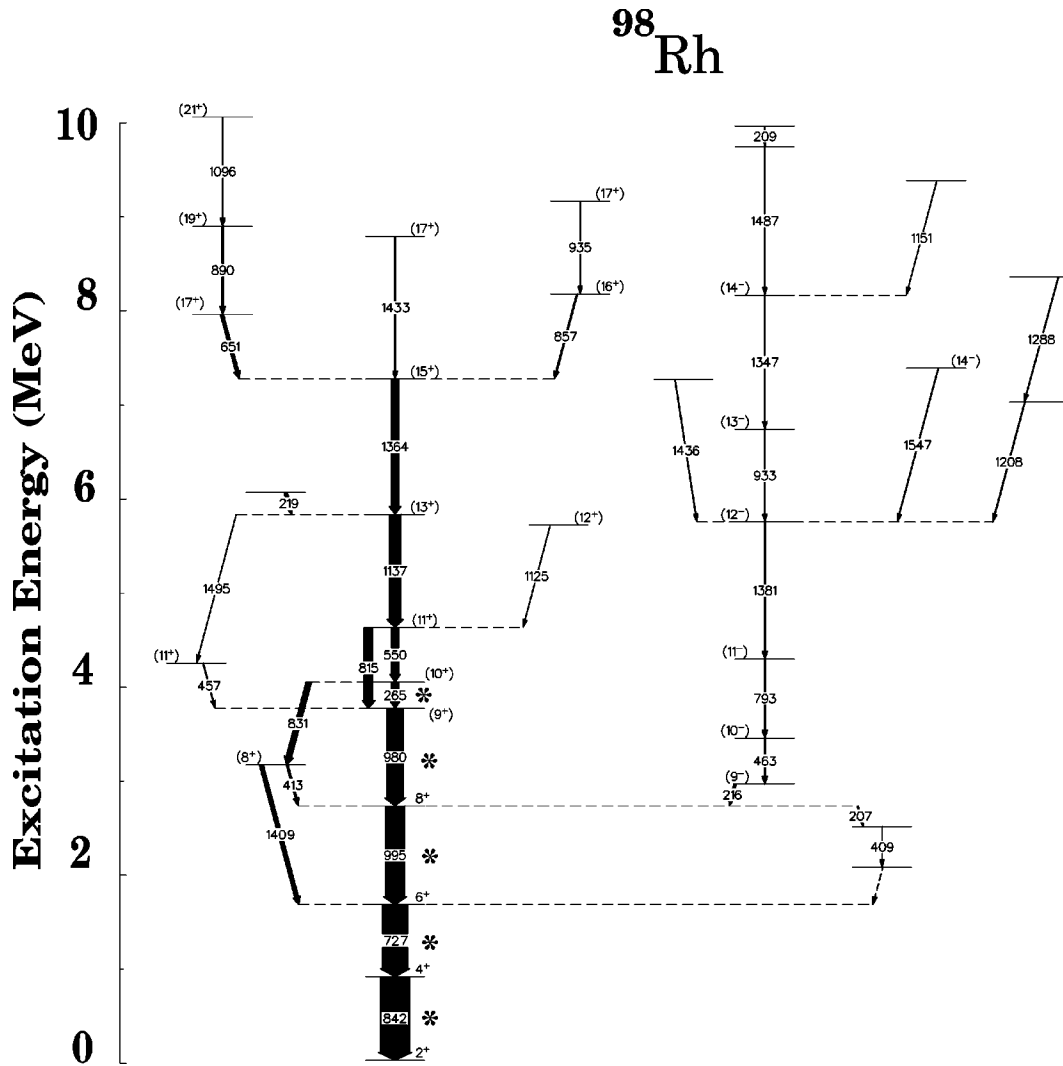


FIG. 4. Level scheme for ^{98}Rh as obtained from the present study. The transition energies are labeled in keV. The previously known transitions are marked with an asterisk. The widths of the arrows are approximately equal to the relative intensities of the observed γ transitions.

nucleus, compared with a total of $\approx 30 \times 10^6$ twofold coincidence events reported in the experiment of Ref. [15], with the intensity of ^{98}Rh approximately 10%.) These transitions do not have consistent coincidence relationships in our data set and do not appear to belong to ^{98}Rh . As shown in Fig. 5, these $E2$ and $M1$ transitions do not appear in coincidence with γ rays in ^{98}Rh . In fact, each of them appears in coincidence with different transitions in nuclei other than ^{98}Rh , which are also populated in our experiment. Therefore, the reported “deformed” band in this nucleus cannot be confirmed in the present work.

IV. DISCUSSION

In our previous work, low-lying levels of the $N = 52$ isotones, such as ^{96}Ru [5] and ^{94}Mo [6], have been interpreted in terms of the spherical shell model. This provides a good starting point in attempting to describe the observed level sequences in ^{97}Rh ($N=52$) as well. The shell model calculations were carried out for this nucleus within the model space code named GL in the OXBASH code [16], encompassing the $\pi(p_{1/2}, g_{9/2})$ and $\nu(d_{5/2}, s_{1/2})$ orbits outside

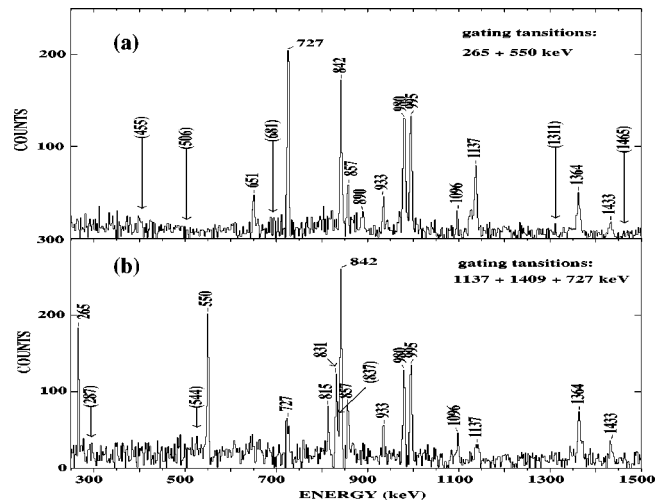


FIG. 5. Double-gated coincidence γ spectra showing the lack of evidence for the “rotational” $E2$ cascade in ^{98}Rh proposed in Ref. [15]. The gating transitions are 265 and 550 keV in the upper panel (a) and 727, 1137, and 1409 keV in the lower panel (b). These spectra have not been corrected for efficiencies of the Ge detectors.

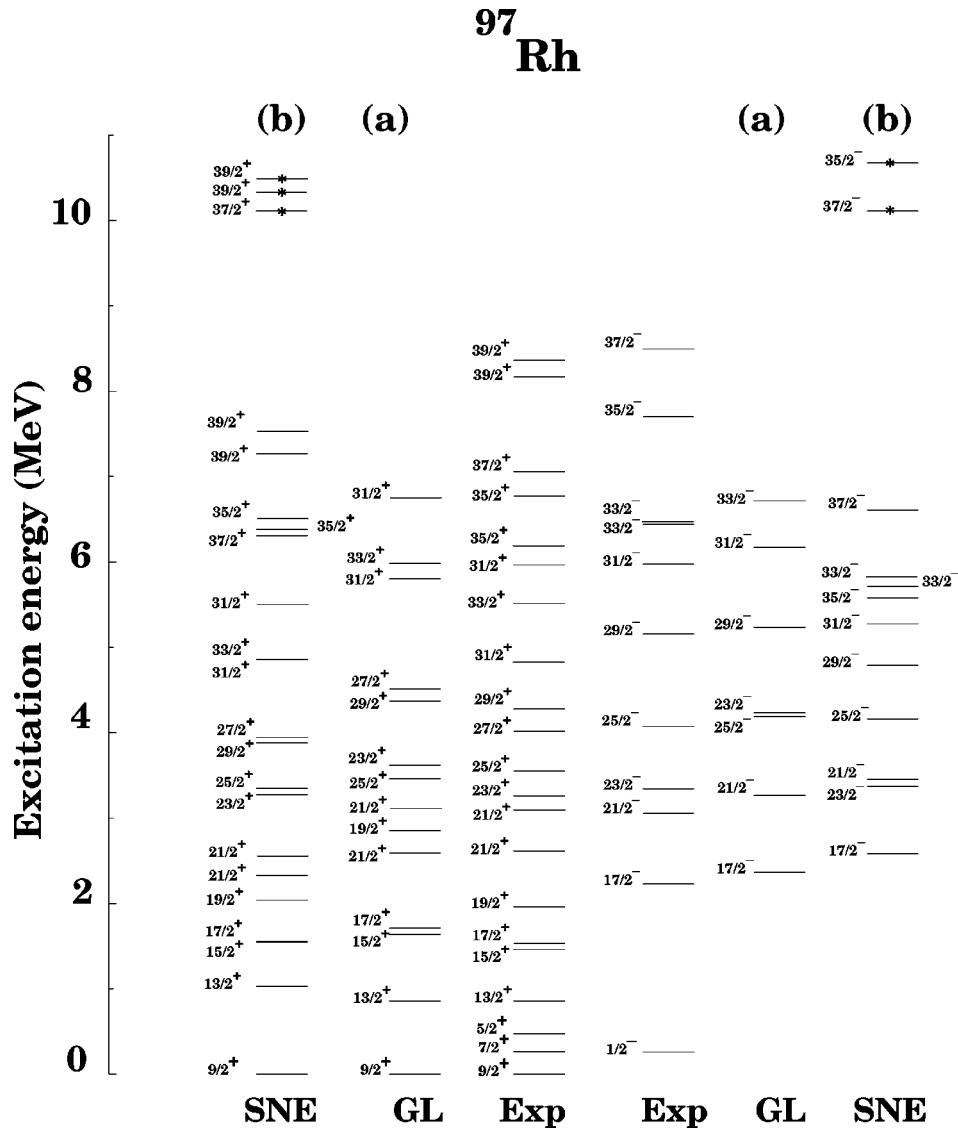


FIG. 6. Comparison of the observed excitation energies in ^{97}Rh with the shell model calculations. See the text for details on the various model spaces (GL and SNE) used.

the ^{88}Sr inert core. The two-body matrix elements were taken from the work of Gloeckner [17]. Within this restricted model space, the maximum angular momentum possible for ^{97}Rh with seven valence protons and two valence neutrons outside the ^{88}Sr inert core is $J=(33/2)\hbar$. As can be seen from Fig. 6(a), there is reasonable agreement between the shell model calculations and the experimental results. However, several discrepancies are observed: (i) The calculations lead to a much larger gap between the levels with spin $31/2^+$ and $27/2^+$ than seen in the experiment; (ii) the predicted excitation energies for the $J=19/2^+$, $23/2^+$, $27/2^+$, and $31/2^+$ states are higher than the observed values [this is most likely indicative of strong admixtures in these states from competing configurations based on the excitation of neutrons into the higher-lying $\nu(g_{7/2}, d_{3/2}, h_{11/2})$ orbits]; and (iii) there is considerable disagreement between the calculations and the experiment for levels at higher angular momenta, suggesting that the restricted model space is no longer appropriate in describing the higher spins. This is not dissimilar to the results reported in Refs. [5,6] where it was suggested that this discrepancy may be attributed, at least in part, to contri-

butions from configurations not incorporated in this restricted model space.

The level scheme of ^{97}Rh shows the presence of γ rays with energies ≥ 1.5 MeV at $J \approx 33/2$. These high-energy transitions are absent at lower spins and appear in parallel with each other at the maximum spin possible from the available orbitals without breaking the core. This suggests a major change in the intrinsic configuration of the higher levels, where a breaking of the $N=50$ core occurs and excitation of the $g_{9/2}$ neutron across the shell gap plays an important role. The various branches seen after the core breaking could be attributed to configurations such as $\pi(p_{1/2}, g_{9/2}) \otimes \nu[(g_{9/2})^{-1}, (d_{5/2})^{+1}]$, or $\pi(p_{1/2}, g_{9/2}) \otimes \nu[(g_{9/2})^{-1}, (g_{7/2})^{+1}]$, or $\pi(p_{1/2}, g_{9/2}) \otimes \nu[(g_{9/2})^{-1}, (h_{11/2})^{+1}]$. A similar feature has been reported by Kharraja *et al.* in the isotone ^{96}Ru [5].

Shell model calculations for ^{97}Rh have been performed, therefore, with an extended model-space encompassing the aforementioned configurations. These calculations are, in effect, identical to those for $^{96,97}\text{Ru}$, and $^{94,95}\text{Mo}$ and have been described in detail previously [5]. Proton excitations

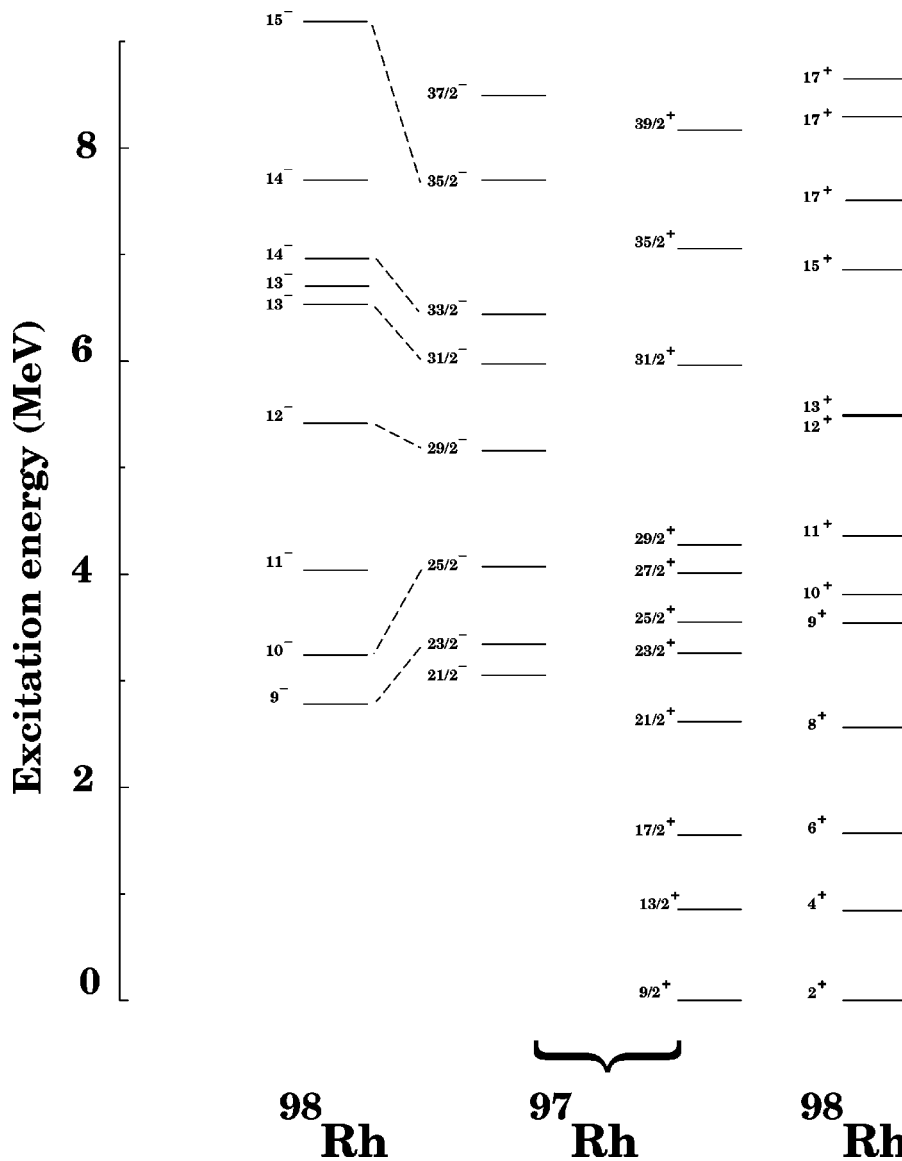


FIG. 7. Comparison of the experimental energy levels of ^{97}Rh and ^{98}Rh assuming the $[^{98}\text{Rh}(J) = ^{97}\text{Rh}(J') \otimes \nu(d_{5/2})]$ stretched configuration.

within the $p_{1/2}, g_{9/2}$ orbits and neutron excitations within the $g_{7/2}, d_{5/2}, d_{3/2}, s_{1/2}, h_{11/2}$ orbits were considered for states with $J \leq 35/2^+, 33/2^-$; no neutron excitation across the $N=50$ closed shell was allowed and the $\pi(f_{5/2}, p_{3/2})$ orbits were completely occupied. For the $J \geq 37/2^+, 35/2^-$ states, the $\nu[(g_{9/2})^{-1} \otimes (d_{5/2})^{+1}]$, $\nu[(g_{9/2})^{-1} \otimes (g_{7/2})^{+1}]$, and $\nu[(g_{9/2})^{-1} \otimes (s_{1/2})^{+1}]$ configurations were incorporated to explore the possibility that these states are dominated by the excitation of a $g_{9/2}$ neutron across the $N=50$ magic core. Due to large dimensions of the m subspace, calculations incorporating the $\nu[(g_{9/2})^{-1} \otimes (h_{11/2})^{+1}]$ configurations could not be carried out.

Figure 6(b) presents the comparison between the experimental and calculated levels for ^{97}Rh using the extended model space described above (code named SNE in OXBASH [16]). The levels labeled by an asterisk were calculated by incorporating the $\nu(g_{9/2})^{-1}$ configurations. The agreement between the shell model predictions and the experimental excitation energies is quite reasonable for levels with $J \leq 35/2^+, 29/2^-$. In particular, there is a considerable im-

provement in the agreement between the shell model predictions and the experimental values for the $19/2^+, 23/2^+, 27/2^+$ and $31/2^+$ states, implying that the structure of these levels does involve the $\pi(p_{1/2}, g_{9/2}) \otimes \nu(d_{5/2}, g_{7/2}, h_{11/2})$ configurations. Indeed, the wave functions for these states are dominated by the $\{\pi[(p_{1/2})^2, (g_{9/2})^5] \otimes \nu[(d_{5/2})^1, (g_{7/2})^1]\}$ and $\{\pi[(p_{1/2})^0, (g_{9/2})^7] \otimes \nu[(d_{5/2})^2, (g_{7/2})^0]\}$ configurations. The agreement for levels with $J \geq 37/2^+, 35/2^-$ is, however, still far from satisfactory. Plausible reasons for this discrepancy could be either the truncation of the model space (certain dominant configurations were not included in this calculations, for example, the $\nu[(g_{9/2})^{-1} \otimes (h_{11/2})^{+1}]$ configuration) or the two-body matrix elements used (for more details see the detailed discussion presented in Ref. [5]).

A cascade of four $E2$ transitions built on the ground-state level (2^+) in ^{98}Rh has been known for some time [14]. However, the spin assignment for the ground state was tentative [18,19]. Gasior *et al.* [19] had assigned spin and parities for the low-lying levels in ^{98}Rh observed from the β decay of ^{98}Pd and $J^\pi = 2^+$ was assigned to the ground state of

^{98}Rh . This assignment was attributed to the $\pi[(g_{9/2})^5] \otimes \nu[(d_{5/2})^{(3-n)}, (s_{1/2})^n]$ configurations, where $n=0,1,2$. The observed isomeric transition retardation factors in ^{98}Rh [20] also supported these single-particle configurations. The shell-model, then, would be a natural choice to attempt to interpret the observed level structure in this nucleus. These calculations have been performed using the GL model space described earlier. Neither the low-lying levels observed by Gasior and co-workers [19] nor the level sequences observed in this study could be reproduced by this restricted GL model space. Since the calculations using the GL model space and the two-body interaction taken from the work of Gloeckner [17] have been able to reproduce rather well the observed level sequences of ^{97}Rh ($N=52$) and of the isotones ^{97}Ru [5] and ^{95}Mo [6], it is remarkable that the present calculations, employing the same set of single particle energies, model space, and effective interactions, fail in ^{98}Rh . A detailed investigation of the possible reasons for this failure is beyond the scope of this paper, but is clearly warranted. One possibility for this discrepancy could be that this nucleus has a low-lying isomeric state with $J^\pi=7^+$, as expected from the coupling of a $9/2^+$ proton ($Z=45$) with a $5/2^+$ neutron ($N=53$), as also from systematics in this region (the ground state of the neighboring $N=53$ isotone, ^{96}Tc , for example, has been assigned these quantum numbers). Such a state would have a rather long half-life and may decay by a low-energy γ transition that could be easily overlooked in our in-beam studies wherein high-spin states are preferentially populated. Remarkably, if $J^\pi=7^+$ is assumed for the lowest level observed in our studies, the excitation energies of the previously known transitions can be reproduced reasonably well by calculations. Of course, in this case all observed levels would have spins higher by $5\hbar$ units.

The weak-coupling scheme is also a recurring theme in the $N=50$ region [21,22] and has been quite successful in explaining the low-lying states of the $N=53$ isotones ^{97}Ru [5] and ^{95}Mo [6]. The same coupling was also very successful in reproducing higher-spin states in ^{95}Ru [2]. Figure 7

shows the results for ^{98}Rh from a stretched coupling scheme where a $d_{5/2}$ neutron is coupled to the ^{97}Rh core, [$^{98}\text{Rh}(J')=^{97}\text{Rh}(J) \otimes \nu(d_{5/2})$]. As can be seen in the figure, the observed level structure of ^{98}Rh , up to a spin of $J \leq 10\hbar$, can be qualitatively understood as [$^{98}\text{Rh}(J)=^{97}\text{Rh}(J')-5/2$]. This simple model does not reproduce the level structure above $J=10\hbar$, however. This discrepancy is likely attributable to the difference in the intrinsic configuration/structure of these states, as compared to the corresponding levels in ^{97}Rh .

V. SUMMARY

High-spin states of $^{97,98}\text{Rh}$ have been identified and the level structures of these nuclei have been extended (up to $J=[(39/2^+), (37/2^-)]$ and $E_x \approx 8$ MeV in ^{97}Rh , and $J=[(21^+), (15^-)]$, $E_x \approx 10$ MeV in ^{98}Rh). The level sequences observed in ^{97}Rh have been interpreted in terms of the spherical shell model. Levels up to $J \leq 35/2^+, 31/2^-$ are dominated by the excitations of the neutrons within the $(g_{7/2}, d_{5/2}, h_{11/2})$ orbitals. The observation of γ rays with $E_\gamma \approx 1.8$ MeV and the fragmentation of intensity into several branches above the $J \approx 37/2^+$ indicate that core breaking occurs at that point, with the states above dominated by the excitation of a $g_{9/2}$ neutron across the $N=50$ shell. Levels in ^{98}Rh up to $J=10\hbar$ can be interpreted in terms of the weak coupling of a $d_{5/2}$ neutron to the ^{97}Rh core. No clear evidence of deformed structures has been found in these nuclei.

ACKNOWLEDGMENTS

The authors would like to acknowledge the help received from B. Prause, Dr. G. Smith, and the Gammasphere support staff during the experiment. This work was supported in part by the U.S. National Science Foundation (Grant No. PHY94-02761), the U.S. Department of Energy (Contract Nos. W-31-109-ENG-38 and DE-FG05-87ER40361), and the Polish-American Maria Sklodowska-Curie Joint Fund II (Project No. PAA/DOE-93-153).

-
- [1] H. A. Roth, S. E. Arnell, D. Foltescu, O. Skeppstedt, J. Blomqvist, A. Nilsson, T. Kuroyanagi, S. Mitarai, and J. Nyberg, *Phys. Rev. C* **50**, 1330 (1994).
- [2] S. S. Ghugre, S. B. Patel, M. Gupta, R. K. Bhowmik, and J. A. Sheikh, *Phys. Rev. C* **50**, 1346 (1994).
- [3] J. Gizon, D. Jerrestam, A. Gizon, M. Jozsa, R. Bark, B. Fogelberg, E. Ideguchi, W. Klamra, T. Lindblad, S. Mitarai, J. Nyberg, M. Piiparinen, and G. Sletten, *Z. Phys. A* **345**, 335 (1993).
- [4] R. P. Singh, S. S. Ghugre, R. K. Bhowmik, M. Gupta, S. Muralithar, S. B. Patel, and G. O. Rodriguez, in *Proceedings of the International Workshop on Physics with Recoil Separators and Detector Arrays, New Delhi, 1995*, edited by R. K. Bhowmik and A. K. Sinha (Allied Publishers, New Delhi, India, 1995), p. 560.
- [5] B. Kharraja, S. S. Ghugre, U. Garg, R. V. F. Janssens, M. P. Carpenter, B. Crowell, T. L. Khoo, T. Lauritsen, D. Nisius, W. Reviol, W. Mueller, L. L. Riedinger, and R. Kaczarowski, *Phys. Rev. C* **57**, 83 (1998).
- [6] B. Kharraja, S. S. Ghugre, U. Garg, R. V. F. Janssens, M. P. Carpenter, B. Crowell, T. L. Khoo, T. Lauritsen, D. Nisius, W. Reviol, W. Mueller, I. L. Riedinger, and R. Kaczarowski, *Phys. Rev. C* **57**, 2903 (1998).
- [7] S. S. Ghugre, B. Kharraja, U. Garg, R. V. F. Janssens, M. P. Carpenter, B. Crowell, T. L. Khoo, T. Lauritsen, D. Nisius, W. Reviol, W. Mueller, L. L. Riedinger, and R. Kaczarowski (unpublished).
- [8] D. C. Radford, *Nucl. Instrum. Methods Phys. Res. A* **361**, 297 (1995).
- [9] J. A. Kuehner, J. C. Waddington, and D. Prevost, in *Proceedings of the International Conference on Nuclear Structure at High Angular Momentum*, Ottawa, 1992, edited by J. C. Waddington and D. Ward, Report No. AECL-10613, 1992 (unpublished), p. 413.
- [10] G. Palameta and J. C. Waddington, *Nucl. Instrum. Methods Phys. Res. A* **234**, 476 (1985).
- [11] B. Crowell, M. P. Carpenter, R. G. Henry, R. V. F. Janssens,

- T. L. Khoo, T. Lauritsen, and D. Nisius, Nucl. Instrum. Methods Phys. Res. A **355**, 575 (1995).
- [12] W. F. Piel, Jr., G. Scharff-Goldhaber, C. J. Lister, and B. J. Varely, Phys. Rev. C **33**, 512 (1986).
- [13] J. Vanhorenbeeck, P. Duhamel, P. Del Marmol, P. Fettweis, and K. Heyde, Nucl. Phys. **A408**, 265 (1983), and references therein.
- [14] M. Behar, A. M. J. Ferrero, A. Filevich, and A. O. Macchiavelli, Z. Phys. A **314**, 111 (1983).
- [15] S. Chattopadhyay, A. Mukherjee, U. Datta Pramanik, A. Goswami, S. Bhattacharya, B. Dasmahapatra, S. Sen, H. C. Jain, and P. K. Joshi, Phys. Rev. C **57**, 471 (1998).
- [16] B. A. Brown, A. Etchegoyen, W. D. M. Rae and N. S. Godwin, MSU-NSCL Report No. 524, 1985 (unpublished).
- [17] D. H. Gloeckner, Nucl. Phys. **A253**, 301 (1975).
- [18] C. M. Lederer, J. M. Hollander, and I. Perlmann, *Table of Isotopes* (Wiley, New York, 1978).
- [19] M. Gasior, A. W. Potempa, H. Roth, and J. Sieniawski, Acta Phys. Pol. B **3**, 153 (1972).
- [20] J. Sieniawski, Acta Phys. Pol. B **5**, 549 (1974).
- [21] M. Behar, A. Ferrero, A. Filevich, G. Garcia Bremudez, and M. A. J. Mariscotti, Nucl. Phys. **A373**, 483 (1982).
- [22] B. A. Brown and D. B. Fossan, Phys. Rev. C **15**, 2044 (1977).